

Ethanol oxidation reaction at Pd-modified nickel foam obtained by PVD method

Tomasz Mikołajczyk, Marcin Turemko, Bogusław Pierozynski*

University of Warmia and Mazury in Olsztyn, Department of Chemistry, Faculty of Environmental Management and Agriculture, Plac Łódzki 4, 10-957 Olsztyn, Poland

*Corresponding author: e-mail: bog.pierozynski@yahoo.ca; boguslaw.pierozynski@uwm.edu.pl

In this study, palladium-modified nickel foam substrate was applied to examine ethanol oxidation reaction (EOR) in 0.1 M NaOH supporting solution. An EOR catalyst was prepared by physical vapour deposition (PVD) of palladium onto Ni foam material. Temperature-dependent kinetics of the EOR were studied over the temperature range: 20–60°C by means of a.c. impedance spectroscopy and cyclic voltammetry techniques. Deposition of a noble metal additive was clearly exposed through scanning electron microscopy: SEM/EDX-supported analysis. Most importantly, this work investigated the effect of pre-deposited fullerene on nickel foam, on the catalytic (EOR) properties of such-produced Ni foam/Pd composite material.

Keywords: PVD, Nickel foam, Electrochemical impedance spectroscopy.

INTRODUCTION

Direct ethanol fuel cells (DEFCs), in which ethyl alcohol is directly used as a fuel have recently attracted a great deal of attention. This is primarily because of their potential suitability for portable applications, but also due to unique properties of C₂H₅OH. Ethanol is considered a promising substitute for methanol, due to its higher (by ca. 30%) energy-density and non-toxic properties. In fact, ethanol is also a renewable resource, as it can be generated from a variety of available agricultural products and biomass substrates^{1–3}. As kinetics of ethanol oxidation process were found to become facilitated in alkaline environments^{4–8}, potential utilization of nickel-based, high surface area electrode materials (having superior corrosion resistance in basic electrolytes), such as Ni foams in the EOR became a technologically viable option. Although Ni foams themselves do not possess catalytic properties towards EOR, they could easily be modified by trace amount of noble elements to produce highly electroactive catalyst composites^{9–13}.

Physical vapour deposition (PVD) processes are atomized deposition technologies, in which material is vaporized from a solid or liquid source in the form of atoms or molecules and transported to the surface, where it condenses. PVD methods are used to deposit thin films of elements or alloys onto various substrate surfaces, e.g. metallic or semiconductor wafers. Key advantages of the PVD technology involve superior film homogeneity and grain size distribution, which typically results in advanced corrosion resistance and mechanical durability, as compared to those exhibited by electro- or chemical deposition methods^{14–18}.

In this work, Pd-modified Ni foam catalyst samples were prepared by the PVD method on nickel foam with pre-deposited fullerene. The role of fullerene was primarily in providing large and homogeneous surface area of the baseline material for subsequent deposition of palladium nanoparticles. Such-obtained catalyst sample materials were then employed as an anode catalyst for the EOR, examined over the temperature range: 20–60°C in 0.1 M NaOH supporting electrolyte.

EXPERIMENTAL

An electrochemical cell made all of Pyrex glass was used during the course of this work. Measurements were carried-out using a conventional three-electrode system, where: a Ni foam-based working electrode (WE) in a central part, a reversible Pd (0.5 mm diameter, 99.9% purity, Aldrich) hydrogen electrode (RHE) as reference and a Pt (1.0 mm diameter, 99.9998% purity, Johnson Matthey, Inc.) counter electrode (CE), both placed in separate compartments were employed. Nickel foam substrate material was provided by MTI Corporation (purity: > 99.99% Ni; thickness: 1.6 mm; surface density: 346 g m⁻²; porosity: ≥ 95%), where all examined electrodes were 1 cm × 2 cm. PVD-modification of Ni foam samples by palladium (carried-out from Pd acetate salt) was made by means of NA-360P vacuum metallization system, where a vacuum chamber was under a dynamic pressure of 10⁻⁵ bar. Before deposition of palladium, Ni foam surface was coated with fullerene to provide extended catalytical surface area, see Refs. 17 and 18. SEM/EDX spectroscopic analysis of Pd-modified nickel foam electrodes was performed by means of Hitachi S3400 SEM/EDX equipment.

Cyclic voltammetry and electrochemical impedance spectroscopy techniques were employed in this work, where all experiments were recorded over the temperature range: 20–60°C by means of *Solatron* 12.608 W Full Electrochemical System. Data analysis was performed with *ZView 2.9* (*Corrview 2.9*) software package, whereas the impedance spectra were fitted using a complex, non-linear, least-squares imittance fitting program *LEVM 6*, written by J.R. Macdonald¹⁹. All other details associated with pre-treatments applied to electrochemical cell and electrodes, preparation of supporting electrolyte (0.25 M C₂H₅OH in 0.1 M NaOH), and employed a.c. impedance protocol were previously described in Refs. 7 and 8.

RESULTS AND DISCUSSION

A SEM micrograph picture of the Pd-modified (by means of the PVD method described in Experimental section) Ni foam material (recorded at 3.500× magnification) is shown in Figure 1a. An amount of Pd

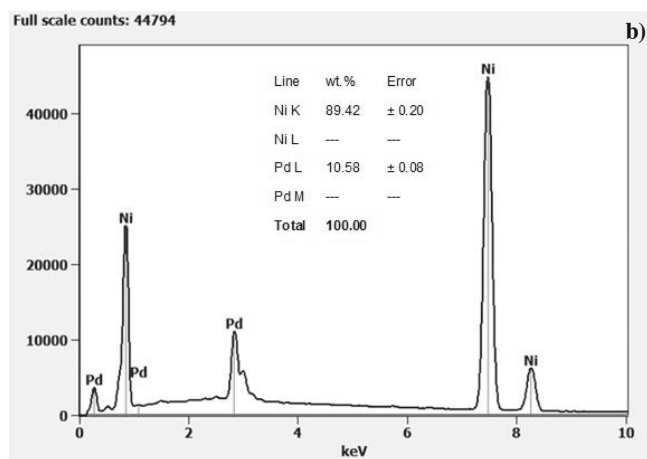
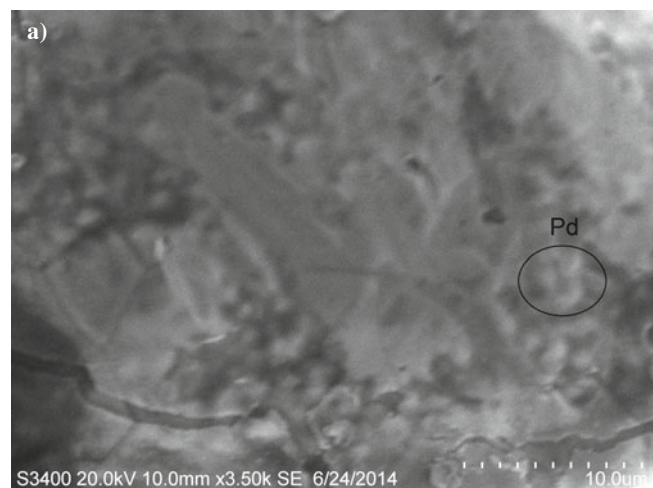


Figure 1. a) SEM micrograph picture of PVD-Pd-modified Ni foam surface (*ca.* 0.42 wt.% Pd), taken at 3.500 \times magnification; b) EDX spectrum for PVD-Pd-modified Ni foam surface along with estimated catalyst composition

loading on the Ni foam substrate was estimated at *ca.* 0.42 wt.% by a weighing method. The Pd detection on the surface of nickel foam was performed by the EDX analysis, carried-out at an acceleration voltage of 20 kV. This confirmed the presence of palladium on the order of 10.58 \pm 0.08 wt.% within the Ni foam/Pd composite (see Fig. 1b), which was dramatically higher than that estimated by the weighing method above. The recorded discrepancy suggests substantial inhomogeneity in the thickness of the PVD-deposited palladium film on the nickel foam surface. In addition, the SEM-approximated Pd grain size value came to 30.0 \pm 5 nm. The above was performed through utilization of the *Image Analysis Program* (NIS-Elements Basic Research on Nikon), based on a similar procedure to that described in detail in Ref. 20.

Cyclic voltammograms of temperature-dependent ethanol oxidation reaction (carried-out in 0.1 M NaOH, at 0.25 M C₂H₅OH), performed on the Pd-modified (by the PVD method) nickel foam surface is shown in Figure 2. Hence, at 20 $^{\circ}$ C, ethanol oxidation starts at *ca.* 0.45 V and maximum of the oxidation current-density is recorded at about 0.80 V. When the CV sweep is reversed towards hydrogen reversible potential, another oxidation peak can be observed at *ca.* 0.62 V. While the high potential oxidation peak corresponds to the formation of other EOR products (e.g. acetaldehyde, acetic acid, etc.), the low potential oxidation peak is typically attributed to the

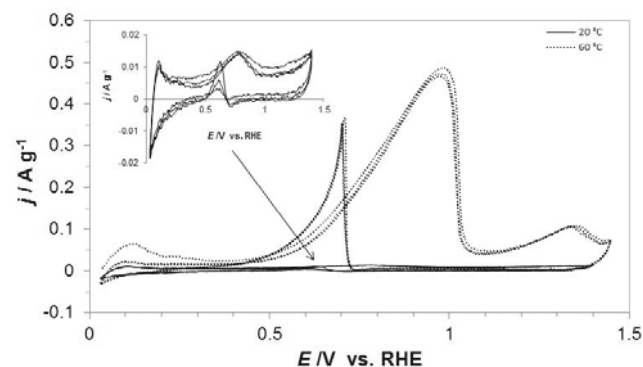


Figure 2. Cyclic voltammograms for ethanol electrooxidation on PVD-Pd-modified Ni foam, carried-out in 0.1 M NaOH at a sweep-rate of 50 mV s⁻¹ and in the presence of 0.25 M C₂H₅OH, at the stated temperature values and additional inset (at 20 $^{\circ}$ C)

surface oxidation of CO_{ads} species^{13, 21-24}. On the other hand, a cyclic voltammetric profile recorded at 60 $^{\circ}$ C exhibited dramatically higher current-densities for the corresponding two voltammetric peaks. Simultaneously, the centre of the high potential peak became radically shifted (by *ca.* 0.50 V) towards more positive potential values (an appropriate correction was introduced in order to account for a small, but significant temperature shift of the Pd RHE²⁵). Moreover, another anodic peak (centred at about 1.34 V) appeared in the CV profile. This peak is most likely associated with further oxidative desorption phenomena²⁶.

Table 1 and Figure 3 below present electrochemical impedance behaviour of the Pd-modified Ni foam electrode. Hence, for 20 $^{\circ}$ C the impedance behaviour is characterized by single and somewhat “depressed” semicircle in the Nyquist impedance plot (see an example in Fig. 3). Here, a CPE-modified simple Randles equivalent model (Fig. 4) was employed to characterize the recorded impedance behaviour. Thus, the recorded reaction resistance, R_{ct} parameter diminished from 692.6 Ω g at 400 mV to reach minimum value of 47.4 Ω g at the potential of 700 mV, which is close to that of the

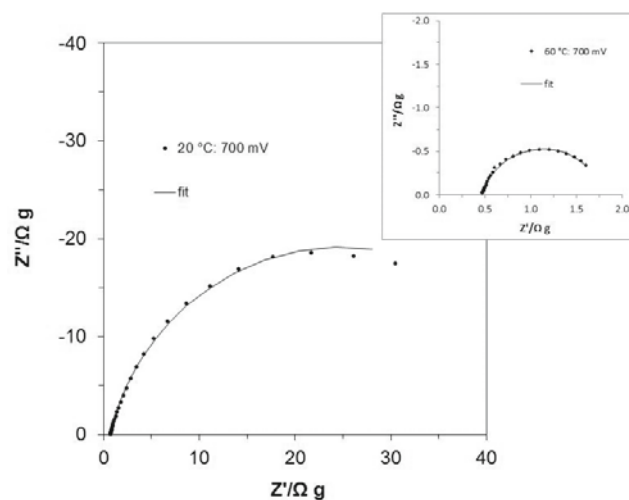
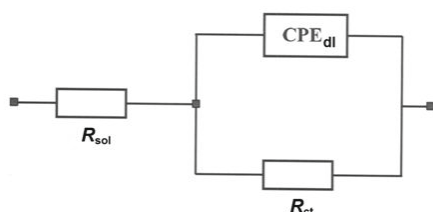


Figure 3. Complex-plane impedance plots for PVD-Pd-modified Ni foam in contact with 0.1 M NaOH, in the presence of 0.25 M C₂H₅OH recorded at 700 mV, at temperatures 20 $^{\circ}$ C and 60 $^{\circ}$ C (inset). The solid line corresponds to representation of the data according to equivalent circuits shown in Figure 4

Table 1. Reaction resistance and interfacial capacitance parameters for electrooxidation of ethanol (at 0.25 M C₂H₅OH) on PVD-Pd-modified Ni foam electrode in 0.1 M NaOH over the temperature range: 20–60°C (also see equivalent circuit in Fig. 4)

E/ mV	20°C	30°C	40°C	50°C	60°C
	$R_{ct}/ \Omega \text{ g}$				
400	692.6 ±83.8	132.0 ±8.9	74.7 ±3.4	44.3 ±1.4	56.3 ±4.2
500	434.8 ±14.9	50.9 ±1.1	14.4 ±0.2	11.6 ±0.1	10.5 ±0.1
600	134.6 ±3.0	11.6 ±0.1	3.1 ±0.0	2.3 ±0.0	2.6 ±0.0
700	47.4 ±0.9	4.4 ±0.0	1.3 ±0.0	1.2 ±0.0	1.3 ±0.0
800	65.2 ±1.6	6.8 ±0.1	0.9 ±0.0	0.9 ±0.0	1.4 ±0.0
900	767.3 ±176.3	27.5 ±0.8	2.1 ±0.0	3.4 ±0.1	13.4 ±0.9
1000	702.1 ±114.9	70.4 ±3.8	20.8 ±0.6	22.6 ±0.6	24.1 ±1.0
1100	809.3 ±153.8	58.7 ±3.2	9.4 ±0.1	7.8 ±0.1	11.1 ±0.3
	$C_{dl}/ \mu\text{F g}^{-1} \text{ s}^{\varphi_1-1}$				
400	15.913 ±98	18.070 ±175	19.207 ±164	17.068 ±176	15.986 ±265
500	12.303 ±73	14.310 ±151	14.433 ±168	13.518 ±170	13.705 ±164
600	12.411 ±107	14.822 ±174	14.005 ±237	13.745 ±153	14.932 ±233
700	14.246 ±158	17.081 ±209	15.874 ±289	16.417 ±299	19.378 ±349
800	20.159 ±105	31.394 ±559	20.551 ±347	23.383 ±420	32.472 ±651
900	22.284 ±192	31.622 ±318	47.986 ±1.763	47.603 ±1.284	41.552 ±743
1000	20.032 ±213	28.226 ±252	31.654 ±393	34.141 ±343	36.135 ±427
1100	21.509 ±246	32.004 ±293	35.310 ±463	39.452 ±586	40.468 ±650

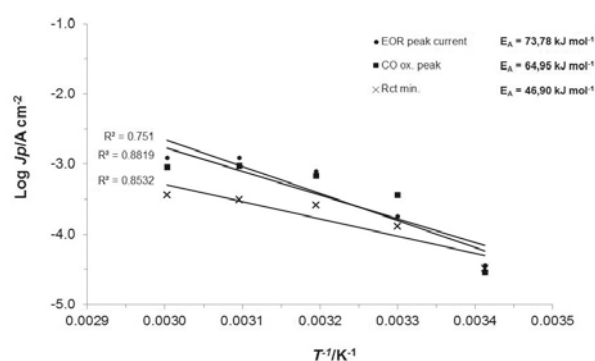
**Figure 4.** CPE-R element equivalent circuit model used for fitting the impedance data for PVD-Pd-modified Ni foam electrode, obtained in 0.1 M NaOH at 0.25 M C₂H₅OH. The circuit includes two constant phase element (CPE) to account for distributed capacitance; R_{ct} and C_{dl} elements correspond to the EOR charge-transfer resistance and double-layer capacitance components, and R_{sol} is solution resistance

peak current-density potential value (see inset to Fig. 2). Then, at increased temperatures significantly reduced values of the R_{ct} parameter were recorded, which at 60°C came to 56.3 and 1.3 $\Omega \text{ g}$, at the potentials of 400 and 700 mV, correspondingly (see Table 1 for details).

On the other hand, the recorded at 20°C double-layer capacitance, C_{dl} parameter exhibited significant fluctuation from 15.913 $\mu\text{F g}^{-1} \text{ s}^{\varphi_1-1}$ at 400 mV to reach 21.509 $\mu\text{F g}^{-1} \text{ s}^{\varphi_1-1}$ at 1100 mV. An increase of the C_{dl} at high potential end implies contribution from surface electro-sorption processes (as pseudocapacitance components), in reference to increased surface concentration of the EOR intermediates. Furthermore, when a commonly used C_{dl} literature value of 20 mF cm⁻² for smooth and homogeneous surfaces^{27, 28} along with electrode mass of 69.8 mg are linked together, an electrochemically active surface area (for a 20°C data series) of the Pd-activated Ni foam could roughly be estimated at 55.6 cm² (at 400 mV) and 77.8 cm² at 900 mV (just prior to the C_{dl} 's rapid increase). In addition, the C_{dl} parameter tends to slightly increase upon temperature rise, being likely a result of electrochemically active surface area extension within the porous structure. Also, in relation to the so-called *capacitance dispersion effect*^{29, 30}, the recorded values of dimensionless parameter φ_1 (for the CPE components in Fig. 4) oscillated between 0.65 and 0.90.

Finally, the Arrhenius plot-derived (see Fig. 5 below) apparent activation energy (E_A) for ethanol electrooxi-

dation on the Pd-modified Ni foam catalyst material was derived for the three selected potentials, namely: EOR peak-current, CO oxidation peak-current and minimum of the R_{ct} parameter. The recorded values of the E_A approached 73.8, 64.9 and 46.9 kJ mol⁻¹, respectively, which was not in a good agreement with those recently presented E_A s for Pd/C composites²⁴ or Pd-bulk^{31, 32} (25.7 to 29.2 kJ mol⁻¹) EOR catalysts. The above was probably caused by inhomogeneous deposition of fullerene layer on the Ni foam surface, which could locally create increased resistances between the background surface and the catalyst's particles. As a result, distribution of fullerene-deposited Pd nano-particles (with an average size of *ca.* 30 nm) on the surface of the background material would be very non-uniform, thus leading to inferior electrocatalytic properties of such-produced composite anode.

**Figure 5.** Arrhenius plots for ethanol electrooxidation (at 0.25 M C₂H₅OH) on PVD-Pd-modified Ni foam electrode in contact with 0.1 M NaOH recorded for the three stated potential values

CONCLUSIONS

PVD-palladium-modified (at about 0.42 wt.% Pd) nickel foam proved to possess some catalytic properties towards electrooxidation of ethanol in 0.1 M NaOH supporting solution, where the EOR kinetics were highly dependent on the reaction temperature.

The recorded values of apparent activation energy for the EOR on PVD-Pd-activated nickel foam were signi-

ificantly higher than those reported in literature under analogous experimental conditions for Pd/C or Pd-bulk type catalysts. In order to improve electrocatalytic EOR behaviour of PVD-Pd-modified (via fullerene deposition as an intermediate stage) Ni foam catalyst one should strive to homogenize the background surface through pre-treatment procedures (e.g. chemical reduction of surface oxide species), as well as by improving the method for fullerene deposition to achieve a uniform carbon layer on the foam surface.

LITERATURE CITED

- Suo, Y. & Hsing, I.M. (2011). Highly active rhodium/carbon nanocatalysts for ethanol oxidation in alkaline medium. *J. Power Sources* 196, 7945–7950. DOI: 10.1016/j.jpowsour.2011.05.048.
- Song, S.Q., Zhou, W.J., Zhou, Z.H., Jiang, L.H., Sun, G.Q., Xin, Q., Leontidis, V., Kontou, S. & Tsiakaras, P. (2005). Direct ethanol PEM fuel cells: The case of platinum based anodes. *Int. J. Hydrogen Energy* 30, 995–1001. DOI: 10.1016/j.ijhydene.2004.11.006.
- Spinace, E.V., Linardi, M. & Neto, A.O. (2005). Co-catalytic effect of nickel in the electro-oxidation of ethanol on binary Pt–Sn electrocatalysts. *Electrochem. Commun.* 7, 365–369. DOI: 10.1016/j.elecom.2005.02.006.
- Dutta, A., Mahapatra, S.S. & Datta, J. (2011). High performance PtPdAu nano-catalyst for ethanol oxidation in alkaline media for fuel cell applications. *Int. J. Hydrogen Energy* 36, 14898–14906. DOI: 10.1016/j.ijhydene.2011.02.101.
- Sheikh, A.M., Correa, P.S., da Silva, E.L., Savaris, I.D., Amico, S.C. & Malfatti, C.F. (2013). Energy conversion using Pd-based catalysts in direct ethanol fuel cell. *RE&PQJ* 11, 300.
- Modibedi, R.M., Masombuka, T. & Mathe, M.K. (2011). Carbon supported Pd–Sn and Pd–Ru–Sn nanocatalysts for ethanol electro-oxidation in alkaline medium. *Int. J. Hydrogen Energy* 36, 4664–4672. DOI: 10.1016/j.ijhydene.2011.01.028.
- Pierozynski, B. (2012). On the Ethanol Electrooxidation Reaction on Catalytic Surfaces of Pt in 0.1 M NaOH. *Int. J. Electrochem. Sci.* 7, 4261–4271.
- Pierozynski, B. (2012). Ethanol Electrooxidation on PtRh and PtRu Catalytic Surfaces in 0.1 M NaOH. *Int. J. Electrochem. Sci.* 7, 6406–6416.
- Mitov, M., Chorbadzhiyska, E., Rashkov, R. & Hubenova, Y. (2012). Novel nanostructured electrocatalysts for hydrogen evolution reaction in neutral and weak acidic solutions. *Int. J. Hydrogen Energy* 37, 16522–16526. DOI: 10.1016/j.ijhydene.2012.02.102.
- Dominguez-Crespo, M.A., Torres-Huerta, A.M., Brachetti-Sibaja, B. & Flores-Vela, A. (2011). Electrochemical performance of Ni–RE (RE = rare earth) as electrode material for hydrogen evolution reaction in alkaline medium. *Int. J. Hydrogen Energy* 36, 135–151. DOI: 10.1016/j.ijhydene.2010.09.064.
- Solmaz, R., Gundogdu, A., Doner, A. & Kardas, G. (2012). The Ni-deposited carbon felt as substrate for preparation of Pt-modified electrocatalysts: Application for alkaline water electrolysis. *Int. J. Hydrogen Energy* 37, 8917–8922. DOI: 10.1016/j.ijhydene.2012.03.008.
- Bidault, F., Brett, D.J.L., Middleton, P.H., Abson, N. & Brandon, N.P. (2009). A new application for nickel foam in alkaline fuel cells. *Int. J. Hydrogen Energy* 34, 6799–6808. DOI: 10.1016/j.ijhydene.2009.06.035.
- Verlato, E., Cattarin, S., Comisso, N., Gambirasi, A., Musiani, M. & Vazquez-Gomez, L. (2012). Preparation of Pd-Modified Ni Foam Electrodes and Their Use as Anodes for the Oxidation of Alcohols in Basic Media. *Electrocatal* 3, 48–58.
- Grum, J. & Sturm, R. (1998). Influence of laser surface melt-hardening conditions on residual stresses in thin plates. *Surf. Coat. Technol.* 100–101, 455–458. DOI: 10.1016/S0257-8972(97)00670-1.
- Navinsek, B., Panjan, P. & Krusic, J. (1998). Hard coatings on soft metallic substrates. *Surf. Coat. Technol.* 98, 809–815. DOI: 10.1016/S0257-8972(97)00316-2.
- Ringleb, F., Sterrer, M. & Freund, H.J. (2014). Preparation of Pd–MgO model catalysts by deposition of Pd from aqueous precursor solutions onto Ag(0 0 1)-supported MgO(0 0 1) thin films. *Applied Catal. A* 474, 186–193. DOI: 10.1016/j.apcata.2013.05.031.
- Czerwosz, E., Diduszko, R., Dluzewski, P., Keczkowska, J., Kozłowski, M., Rymarczyk, J. & Suchanska, M. (2007). Properties of Pd nanocrystals prepared by PVD method. *Vacuum* 82(4), 372–376. DOI: 10.1016/j.vacuum.2007.08.003.
- Diduszko, R., Kowalska, E., Kozłowski, M., Czerwosz, E. & Kaminska, A. (2013). Temperature-induced changes in the topography and morphology of C–nPd films deposited on fused silica. *Optica Applicata XLIII*(1), 133–141. DOI: 10.5277/oa130117.
- Macdonald, J.R. (1987). Impedance spectroscopy, emphasizing solid materials and systems. *New York: John Wiley & Sons.*
- Smoczyński, L., Ratnaweera, H., Kosobucka, M. & Smoczyński, M. (2014). Image analysis of sludge aggregates. *Sep. Purif. Technol.* 122, 412–420. DOI: 10.1016/j.seppur.2013.09.030.
- Xia, X.H., Liess, H.D. & Iwasita, T. (1997). Early stages in the oxidation of ethanol at low index single crystal platinum electrodes. *J. Electroanal. Chem.* 437, 233–240. DOI: 10.1016/S0022-0728(97)00404-X.
- Abd-El-Latif, A.A., Mostafa, E., Huxter, S., Attard, G. & Baltruschat, H. Electrooxidation of ethanol at polycrystalline and platinum stepped single crystals: A study by differential electrochemical mass spectrometry. (2010). *Electrochim. Acta* 55, 7951. DOI: 10.1016/j.electacta.2010.04.008.
- Gomes, J.F., Busson, B., Tadjeddine, A. & Tremilios-Filho, G. (2008). Ethanol electro-oxidation over Pt(hkl): Comparative study on the reaction intermediates probed by FTIR and SFG spectroscopies. *Electrochim. Acta* 53, 6899–6905. DOI: 10.1016/j.electacta.2008.01.054.
- Sun, S., Jusys, Z. & Behm, R.J. (2013). Electrooxidation of ethanol on Pt-based and Pd-based catalysts in alkaline electrolyte under fuel cell relevant reaction and transport conditions. *J. Power Sources* 231, 122–133. DOI: 10.1016/j.jpowsour.2012.12.091.
- Pierozynski, B. (2011). On the Hydrogen Evolution Reaction at Nickel-Coated Carbon Fibre in 30 wt.% KOH Solution. *Int. J. Electrochem. Sci.* 6, 63–77.
- Camara, G.A. & Iwasita, T. (2005). Parallel pathway of ethanol oxidation: The effect of ethanol concentration. *J. Electroanal. Chem.* 578, 315–321. DOI: 10.1016/j.jelechem.2005.01.013.
- Lasia, A. & Rami, A. (1992). Kinetics of hydrogen evolution on Ni–Al alloy electrodes. *J. Applied Electrochem.* 22, 376–382.
- Chen, L. & Lasia, A. (1991). Study of the Kinetics of Hydrogen Evolution Reaction on Nickel-Zinc Alloy Electrodes. *J. Electrochem. Soc.* 138, 3321–3328. DOI: 10.1149/1.2085409.
- Pajkossy, T. (1994). Impedance of rough capacitive electrodes. *J. Electroanal. Chem.* 364, 111–125. DOI: 10.1016/0022-0728(93)02949-I.
- Conway, B.E. & Pierozynski, B. (2008) A.c. impedance behaviour of processes involving adsorption and reactivity of guanidonium-type cations at Pt(100) surface. *J. Electroanal. Chem.* 622, 10–14. DOI: 10.1016/j.jelechem.2008.04.025.
- Wang, D., Liu J., Wu, Z., Zhang, J., Su, Y., Liu, Z. & Xu C. (2009). Electrooxidation of Methanol, Ethanol and 1-Propanol on Pd Electrode in Alkaline Medium. *Int. J. Electrochem. Sci.* 4, 1672–1678.
- Xie, S.W., Chen S., Liu Z.Q. & Xu C.W. (2011). Comparison of Alcohol Electrooxidation on Pt and Pd Electrodes in Alkaline Medium. *Int. J. Electrochem. Sci.* 6, 882–888.